OPTICS

High-harmonic generation in graphene enhanced by elliptically polarized light excitation

Naotaka Yoshikawa,[1,2]* Tomohiro Tamaya,[1]† Koichiro Tanaka[1,2]*

The electronic properties of graphene can give rise to a range of nonlinear optical responses. One of the most desirable nonlinear optical processes is high-harmonic generation (HHG) originating from coherent electron motion induced by an intense light field. Here, we report on the observation of up to ninth-order harmonics in graphene excited by mid-infrared laser pulses at room temperature. The HHG in graphene is enhanced by an elliptically polarized laser excitation, and the resultant harmonic radiation has a particular polarization. The observed ellipticity dependence is reproduced by a fully quantum mechanical treatment of HHG in solids. The zero-gap nature causes the unique properties of HHG in graphene, and our findings open up the possibility of investigating strong-field and ultrafast dynamics and nonlinear behavior of massless Dirac fermions.

High-harmonic generation (HHG) has been intensely investigated in atomic gases for its application to the generation of coherent attosecond radiation in the extreme ultraviolet and soft x-ray regions (*1*, *2*). HHG has been reported in various crystalline solids (*3*–*11*) and described as a probing method of the electronic properties of solids. The mechanism of HHG in solids is fundamentally different from that in atomic gases because of the higher density of the atoms and their periodic structure. In particular, recent reports have revealed that HHG is sensitive to the orientation of the electric field relative to the crystal axis (*9*–*11*). HHG has been demonstrated as a good tool for exploring the nature of the electron systems in crystals in terms of the symmetry of the electronic band structure (*9*), interatomic bonding (*10*), and the material's Berry curvature (*11*). Although this property of HHG clearly reflects the diversity of solids, the diversity it affords may obscure the universal nature of HHG in solids. Several theoretical models have been proposed for solid-state HHG (*3*–*14*), such as interband polarization combined with dynamical Bloch oscillations (*4*, *7*, *9*), intraband electron dynamics (*10*, *11*), and time-dependent diabatic process (*12*); however, a unified predictive theory that captures the essential feature of HHG in solids remains elusive.

In bulk crystals, the essential feature of solid-state HHG may be swept out due to the propagation effects, such as phase matching conditions. It is therefore important to gain an understanding of HHG in simple, two-dimensional material. Graphene is a monolayer of carbon atoms packed in a two-dimensional honeycomb lattice, and it exhibits a unique band structure with a zero energy gap and linear energy dispersion, the Dirac cone (*15*, *16*). The important characteristic here is that the band structure of graphene relevant to HHG is isotropic even in the visible region. An HHG experiment in graphene should capture the universal properties of HHG in solids independently of the crystal angle and provide a standard test case for checking the validity of proposed theories.

The band structure of graphene gives rise to several remarkable properties, including universal conductivity (*17*–*19*). Linear energy dispersion also gives a fixed group velocity that is only dependent on the direction of the k vector, leading to a strongly nonlinear electromagnetic response. Although the semiclassical model (*20*) and quantum mechanical theory (*21*) each predict HHG, there has been no report of observation of HHG in monolayer graphene. Fifth-harmonic generation in the terahertz (THz) region was demonstrated in 45-layer graphene (*22*); however, its efficiency of third-harmonic generation was quite low in contrast with the theoretical prediction (*23*). The low efficiency should come from the extraordinarily fast relaxation of electrons (*24*–*28*) that prohibits coherent optical processes in the THz frequency region. Because of this problem, attention has shifted to devising an HHG experiment with mid-infrared light.

A typical high-harmonic (HH) spectrum is shown (Fig. 1B) of monolayer graphene excited by linearly polarized mid-infrared (0.26 eV) pulses (Fig. 1A) (*29*). The peak power of the pump pulse was 1.7 TW/cm^2, which corresponds to an electric field 30 MV/cm inside the graphene, taking into account the reflectivity of the substrate. All experiments were performed at room temperature. Odd-order harmonics can be seen up to ninth order. We subtracted the background broad luminescence from impurities or defects insensitive to the photon energy and polarization of the excitation light (fig. S4) (*29*). The intensity of fifth-harmonic radiation as a function of the peak power of the excitation pulse I_{exc} (red circles, Fig. 1C) shows a saturation-like behavior, whereas it should show an I^5 dependence (dashed red line) in the perturbative limit. It scales as I_{exc}^2 (gray line) at the highest pump intensity in this study. The power dependence clearly shows the nonperturbative nature of the HHG process in graphene (*4*, *11*).

Figure 2 shows HH spectra for various polarizations of the pump laser as characterized by ellipticity, defined as $\varepsilon = E_y/E_x$. The peak power of the laser was 0.8 TW/cm^2. The orientation of the variable retarder was fixed, and we controlled the laser ellipticity by changing the retardance in order to keep the major axis of the elliptical polarization fixed. All harmonics vanish when the graphene is pumped by circular polarized light ($\varepsilon = 1$). However, with the elliptically polarized pump ($\varepsilon = 0.32$), the seventh and ninth harmonics are enhanced compared with those having a linearly polarized pump ($\varepsilon = 0$). This is notably different from gas-phase HHG, where the yield of HHG

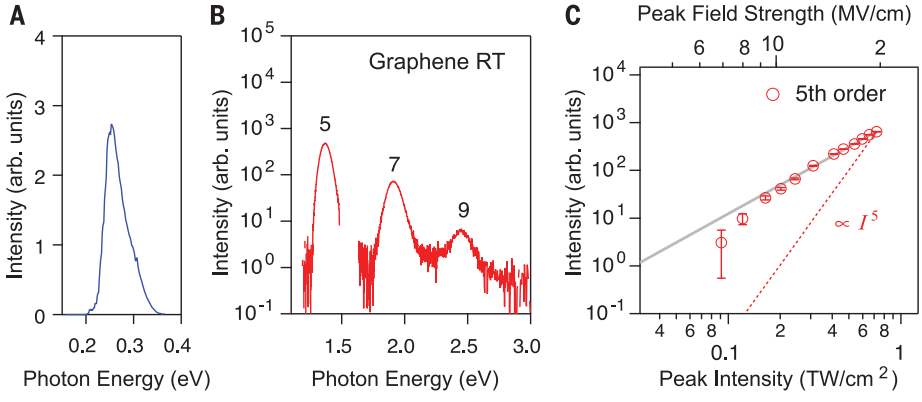

Fig. 1. HHG from graphene. (**A**) The spectrum of the excitation pulse. The full width at half maximum is ~60 meV. (**B**) HH radiation spectrum of graphene (red curve) and spectrum of excitation pulse (blue dotted curve). (**C**) Pump power dependence of intensity of fifth-harmonic radiation.

[1]Department of Physics, Graduate School of Science, Kyoto University, Sakyo-ku, Kyoto 606-8502, Japan. [2]Institute for Integrated Cell-Material Sciences (WPI-iCeMS), Kyoto University, Sakyo-ku, Kyoto 606-8501, Japan.
*Corresponding author. Email: y.naotaka@scphys.kyoto-u.ac.jp (N.Y.); kochan@scphys.kyoto-u.ac.jp (K.T.) †Present address: Nanoelectronics Research Institute (NeRI), National Institute of Advanced Industrial Science and Technology (AIST), Tsukuba, Ibaraki 305-8568, Japan.

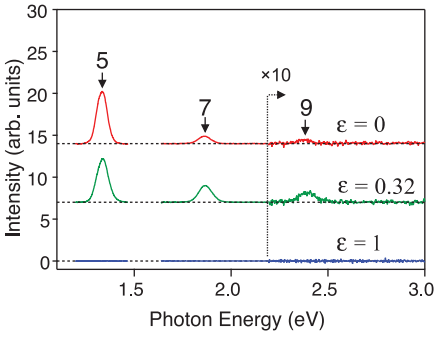

Fig. 2. HH spectra for various laser ellipticities. HH radiation spectra for different ellipticities of the pump laser ε = 0 (red curve), ε = 0.32 (green curve), and ε = 1 (blue curve).

monotonically decreases as the pump ellipticity increases (*30*).

We also investigated the polarization of the HH radiation. Figure 3, A and B, shows simulated polar plots of the laser intensity for the linear polarization (ε = 0) and elliptical polarization (ε = 0.32), respectively, with the major axis of the excitation laser set to the angle 0, that is, the horizontal axis. The normalized polar plots from the experiment confirm that with a linearly polarized pump, the fifth and seventh harmonics also show a linear polarization whose orientation coincides with that of the pump laser. The polarizations of the HH radiation under an elliptically polarized pump are rotated with respect to the major axis of the pump laser and are almost perpendicular to it.

Figure 4B illustrates the detailed ellipticity dependence of the intensity of the seventh-harmonic radiation, where the experimental configuration of polarizations is illustrated in Fig. 4A. The harmonic radiation is divided into two polarization components parallel to the major axis (I_x, red circles) and minor axis (I_y, blue squares) of the laser polarization. The plotted intensities are normalized by I_x at ε = 0. I_x decreases gradually as the ellipticity of the laser increases. I_y is greatly enhanced with elliptically polarized excitations and reaches a maximum value at a finite ellipticity. These results are consistent with the ellipticity dependence of the HH yields in Fig. 2 and the polarization in Fig. 3. The HHG in graphene and its ellipticity dependence are unchanged when the crystal axis is rotated with respect to the major axis of laser polarization, as expected due to the isotropic nature of the Dirac cone.

We found that HHG in graphene is enhanced at a finite laser ellipticity and that its polarization axis is rotated from the major axis of the elliptical polarization. This ellipticity dependence is an essential feature of HHG in graphene. Recent work reported an enhancement of HHG in MgO under elliptical or circular polarized pumps (*10*), in which it was claimed that harmonic efficiency is enhanced for semiclassical electron trajectories that connect neighboring atomic sites in the crystal. In monolayer MoS_2, even-order harmonics were polarized perpendicular to the linearly polarized pump, which was also explained by the semiclassical model, including the anomalous transverse intraband current arising from the material's Berry curvature (*11*). In the case of graphene, however, a fully quantum mechanical model should be used because one-photon resonant excitation can occur at any photon energy of the fundamental light. We investigated the characteristics of HHG in graphene within the framework of the fully quantum mechanical theory that we developed (*12*, *31*). Our theoretical framework uses an external electric field in the form of a vector potential rather than a scalar one; thus, the justification of using Bloch's theorem is ensured even in a high-intensity electric field, where a temporally changing band structure induces motion of the wave packet of the polarization in k space and gives rise to HHG and its polarization dependence. In (*12*), we suggested that the mechanism of HHG in solids can be classified into three regimes: (i) the multiphoton absorption regime, (ii) the ac Zener regime, and (iii) the semimetal regime. It is characterized by the ratio between the Rabi frequency Ω_{R0} and the bandgap E_g, and we found that in the semimetal regime ($E_g/2\hbar \leq \Omega_{R0}$), the yields of the HH radiation reach a maximum value at a certain finite pump field ellipticity and that the perpendicular polarization components with respect to the major axis of the laser are strongly enhanced (*31*). Figure 3B shows I_x and I_y calculated by applying our theory to the linear energy dispersion of electrons in graphene (*29*). The resultant curves reproduce the experimental data, including the intensity ratio of I_x and I_y and the ellipticity at which I_y takes a maximum value. The ellipticity dependence of the intensity and polarization indicates that the HHG process in graphene is in the semimetal regime.

Furthermore, our theory explains the polarization of the HH radiation represented in Fig. 3, C and D. Figure 3, E and F, shows polar plots obtained from the calculation, which describe the polarization of the fifth and seventh harmonics with ε = 0 and ε = 0.3. The calculation reproduces the experimental finding in which the orientation of the HH radiation is rotated under excitation by elliptically polarized light. We also examined the semiclassical model of the HHG in graphene based on the acceleration theorem,

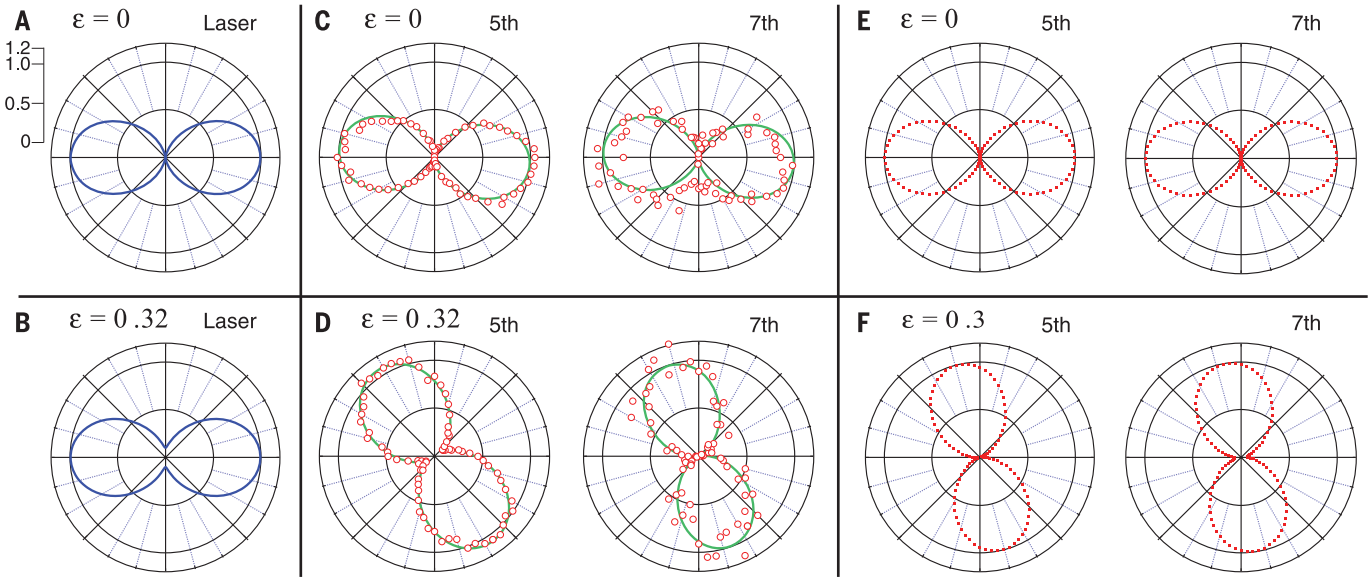

Fig. 3. Polarizations of HH radiation. (**A** and **B**) Simulated polar plots of intensities of the excitation laser with ε = 0 and ε = 0.32. (**C** and **D**) Normalized intensities of the measured fifth and seventh harmonics with ε = 0 and ε = 0.32. Green curves are eye guides. (**E** and **F**) Similar set to (C) and (D) for the theoretical calculation with ε = 0 and ε = 0.3.

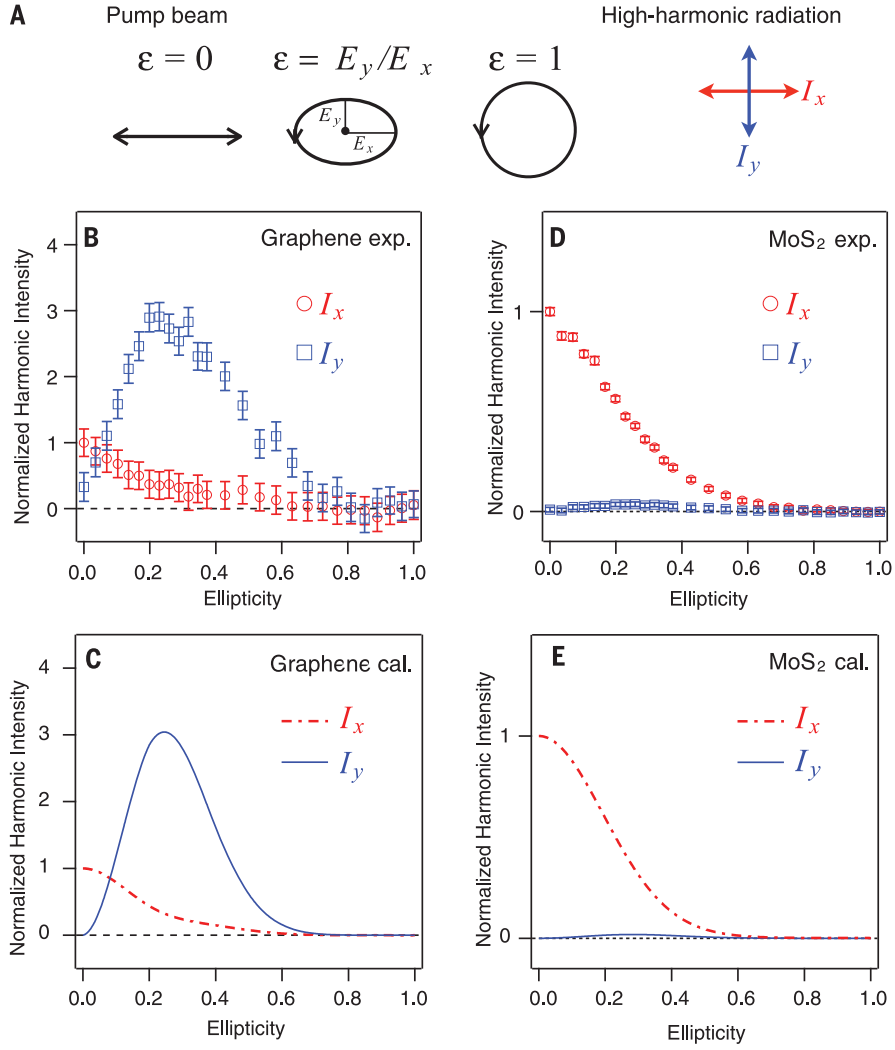

Fig. 4. Ellipticity dependence of HH radiation from graphene and monolayer MoS_2. (**A**) Illustration of polarization configuration of the pump beam and HH radiation. (**B**) Normalized intensities of the seventh-harmonic radiation from graphene as a function of laser ellipticity. (**C**) Theoretical results reproducing the experimental data in (B). (**D** and **E**) The same data set as (B) and (C) for monolayer MoS_2.

but it cannot explain the experimental data (fig. S5) (*29*).

The mechanism of the HHG should depend on the ratio between the Rabi frequency and the bandgap. Because graphene is a gapless material (E_g = 0), the condition of the semimetal regime ($E_g/2\hbar \leq \Omega_{R0}$) can be achieved even with a weak field excitation. As a control study, we performed an HHG experiment and theoretical calculation on monolayer MoS_2 (fig. S6) (*29*), which is an atomically thin material with honeycomb lattice structure like graphene but with a finite bandgap (exciton resonance ~1.85 eV). We set the excitation photon energy and intensity to be the same as those used in the experiments and calculations for graphene. The intensity of the seventh-harmonic radiation monotonically decreases with increasing ellipticity of the laser, and the perpendicular component to the major axis (I_y) is small (Fig. 4D). The calculated curves in Fig. 4E for E_g = 1.85 eV, which corresponds to $E_g/2\hbar > \Omega_{R0}$, reproduce the experimental data for monolayer MoS_2. This indicates that at the current excitation strength, the mechanism of HHG in monolayer MoS_2 is not in the semimetal regime. The calculation for monolayer MoS_2 assumes the band structure with a bandgap of 1.85 eV and parabolic dispersions of the valence and conduction bands with the same form factor as graphene (*29*). The comparative study of HHG in monolayer graphene and monolayer MoS_2 reveals that the mechanism of HHG in solids depends on the bandgap of the material. In the limit of a small bandgap or large Rabi frequency, the mechanism is in the semimetal regime, and the unique ellipticity dependence of HHG appears. We also showed the universality of the ellipticity dependence of HHG for different order harmonics. The HH spectra in Fig. 2 show that not only the seventh but also the ninth harmonic is enhanced with elliptically polarized excitation. The ellipticity dependence for the fifth harmonic is shown in fig. S7 (*29*). It should be noted that not the linear energy dispersion but the zero-gap property of graphene plays an important role in HHG, because we found that the unique ellipticity dependence appears in the calculation even when a parabolic band structure is assumed. The similar nature is expected to appear in narrow bandgap semiconductors such as InSb. Our experimental findings and good agreement with the theoretical calculation strongly suggest that the fully quantum mechanical model that we have developed provides an appropriate model of HHG in solids.

REFERENCES AND NOTES

1. F. Krauzs, M. Ivanov, *Rev. Mod. Phys.* **81**, 163–234 (2009).
2. P. B. Corkum, F. Krausz, *Nat. Phys.* **3**, 381–387 (2007).
3. S. Ghimire *et al.*, *Nat. Phys.* **7**, 138–141 (2011).
4. O. Schubert *et al.*, *Nat. Photonics* **8**, 119–123 (2014).
5. T. T. Luu *et al.*, *Nature* **521**, 498–502 (2015).
6. G. Vampa *et al.*, *Nature* **522**, 462–464 (2015).
7. M. Hohenleutner *et al.*, *Nature* **523**, 572–575 (2015).
8. G. Ndabashimiye *et al.*, *Nature* **534**, 520–523 (2016).
9. F. Langer *et al.*, *Nature* **533**, 225–229 (2016).
10. Y. S. You, D. A. Reis, S. Ghimire, *Nat. Phys.* **13**, 345–349 (2016).
11. H. Liu *et al.*, *Nat. Phys.* **13**, 262–265 (2016).
12. T. Tamaya, A. Ishikawa, T. Ogawa, K. Tanaka, *Phys. Rev. Lett.* **116**, 016601 (2016).
13. T. Higuchi, M. I. Stockman, P. Hommelhoff, *Phys. Rev. Lett.* **113**, 213901 (2014).
14. M. Wu, S. Ghimire, D. A. Reis, K. J. Schafer, M. B. Gaarde, *Phys. Rev. A* **91**, 043839 (2015).
15. K. S. Novoselov *et al.*, *Nature* **438**, 197–200 (2005).
16. Y. Zhang, Y.-W. Tan, H. L. Stormer, P. Kim, *Nature* **438**, 201–204 (2005).
17. T. Ando, Y. Zheng, H. Suzuura, *J. Phys. Soc. Jpn.* **71**, 1318–1324 (2002).
18. N. M. R. Peres, F. Guinea, A. H. Castro Neto, *Phys. Rev. B* **73**, 125411 (2006).
19. R. R. Nair *et al.*, *Science* **320**, 1308 (2008).
20. S. A. Mikhailov, K. Ziegler, *J. Phys. Condens. Matter* **20**, 384204 (2008).
21. K. Ishikawa, *Phys. Rev. B* **82**, 201402 (2010).
22. P. Bowlan, E. Martinez-Moreno, K. Reimann, T. Elsaesser, M. Woerner, *Phys. Rev. B* **89**, 041408 (2014).
23. I. Al-Naib, J. E. Sipe, M. M. Dignam, *Phys. Rev. B* **90**, 245423 (2014).
24. T. Kampfrath, L. Perfetti, F. Schapper, C. Frischkorn, M. Wolf, *Phys. Rev. Lett.* **95**, 187403 (2005).
25. P. A. George *et al.*, *Nano Lett.* **8**, 4248–4251 (2008).
26. J. Dawlaty, S. Shivaraman, M. Chandrashekhar, F. Rana, M. G. Spencer, *Appl. Phys. Lett.* **92**, 042116 (2008).
27. S. Tani, F. Blanchard, K. Tanaka, *Phys. Rev. Lett.* **109**, 166603 (2012).
28. M. J. Paul *et al.*, *New J. Phys.* **15**, 085019 (2013).
29. Supplementary materials are available online.
30. P. Dietrich, N. H. Burnett, M. Ivanov, P. B. Corkum, *Phys. Rev. A* **50**, R3585(R) (1994).
31. T. Tamaya, A. Ishikawa, T. Ogawa, K. Tanaka, *Phys. Rev. B* **94**, 241107(R) (2016).

ACKNOWLEDGMENTS

This work was supported by a Grant-in-Aid for Scientific Research (A) (grant 26247052). N.Y. was supported by a Japan Society for the Promotion of Science fellowship (grant 16J10537).

SUPPLEMENTARY MATERIALS

www.sciencemag.org/content/356/6339/736/suppl/DC1
Materials and Methods
Supplementary Text
Figs. S1 to S7
References (*32*–*34*)

10 February 2017; accepted 25 April 2017
10.1126/science.aam8861

High-harmonic generation in graphene enhanced by elliptically polarized light excitation

Naotaka Yoshikawa, Tomohiro Tamaya and Koichiro Tanaka (May 18, 2017)

Science **356** (6339), 736-738. [doi: 10.1126/science.aam8861]

Editor's Summary

Graphene takes light to a higher level

High harmonic generation is a useful nonlinear effect in which the light-matter interaction within a material results in the conversion of one wavelength to a shorter one. Typically performed in atomic gases, there is now interest in extending such a process to the solid state. Yoshikawa *et al.* pumped single-layer graphene with intense polarized pulses of infrared light to generate ultraviolet light, up to the ninth harmonic. Theoretical analysis of the process suggests that the effect could be transferred to other solid-state systems, providing a possible route to develop coherent light sources across the spectrum.

Science, this issue p. 736

Science (print ISSN 0036-8075; online ISSN 1095-9203) is published weekly, except the last week in December, by the American Association for the Advancement of Science, 1200 New York Avenue NW, Washington, DC 20005.